Nanoscale

RSC Publishing

COMMUNICATION

View Article Online
View Journal | View Issue

Free-standing nitrogen-doped carbon nanofiber films as highly efficient electrocatalysts for oxygen reduction†

Cite this: *Nanoscale*, 2013, **5**, 9528

Dong Liu,[ab] Xueping Zhang,[ab] Zaicheng Sun[c] and Tianyan You*[a]

Received 24th June 2013
Accepted 2nd August 2013

DOI: 10.1039/c3nr03229a

www.rsc.org/nanoscale

Free-standing nitrogen-doped carbon nanofiber (NCNF) films based on polyacrylonitrile (PAN) were prepared simply by the combination of electrospinning and thermal treatment. We reused the nitrogen-rich gas generated as the byproduct of PAN at elevated temperature, mainly NH_3, for surface etching and nitrogen doping. The as-obtained NCNFs exhibited a rougher surface and smaller diameter than pristine carbon nanofibers. Despite the decreased total N content, a significant increase in the content of pyrrolic-N was observed for the NCNFs. In application to electrochemistry, the free-standing NCNF films showed comparable catalytic activity with a close four-electron pathway to a commercial Pt/C catalyst in alkaline medium toward oxygen reduction reaction (ORR), which can be attributed to the nitrogen doping and high hydrophilicity. More importantly, the ORR current density on the NCNFs only dropped 6.6% after 10 000 s of continuous operation, suggesting an enhanced long-time durability. In addition, the NCNFs also showed better electrocatalytic selectivity than Pt/C. Our work reveals a facile but efficient approach for the synthesis of free-standing NCNF films as a promising alternative to Pt-based electrocatalysts in fuel cells.

Introduction

The development of catalytic materials for oxygen reduction reaction (ORR) is one of the major issues in the practical applications of fuel cells.[1] In spite of the outstanding performance of Pt-based ORR electrocatalysts, the commercialization is hampered by the high cost of noble metals and relatively poor durability.[2,3] Recently, the investigation of substitutes for the Pt-based catalysts, including nonprecious metals[4–8] and metal-free catalysts,[9–15] has attracted great interest. In particular, the state-of-the-art metal-free nitrogen-doped carbon nanomaterials, such as nitrogen-doped carbons,[11,12] graphene[13,14] and carbon nanotubes,[15] exhibited excellent electrocatalytic activity and enhanced durability toward the ORR. Their high electrochemical performance could be attributed to the improvement of the interaction between carbon and guest molecules resulting from the enhancement of the electron-donor property of the carbon host.[16] Although significant progress in nitrogen-doped carbon nanomaterials has been made as catalysts for the ORR, there have been few reports on the facile synthesis of nitrogen-doped carbon nanofibers (NCNFs).[17–19] Generally, there are two main approaches for the introduction of nitrogen into the carbon nanofibers (CNFs): one is by introducing the nitrogen into CNFs during the preparation process;[17,18] the other is by the post-treatment of CNFs in the nitrogen-containing gas.[19] Moreover, an insulating binder was required for the powdery materials to stick the samples onto the support materials which results in an unwanted inner resistance, while electrospun NCNFs could be produced with a unique free-standing structure which is expected to retain its high catalytic activity.[20] Hence, it is desirable to develop a simple approach for the efficient production of free-standing NCNF films with high oxygen-reduction activity.

Herein, we report a novel approach for the synthesis of free-standing NCNF films based on electrospun polyacrylonitrile (PAN) nanofibers. For the first time, NH_3-containing gas, which was the byproduct of PAN during the thermal treatment and always discharged as a tail gas, was reused for nitrogen doping and surface etching, leading to the rough surface and small diameter of NCNFs. The electrochemical measurements demonstrated that the as-made NCNF films had high catalytic activity, enhanced long-time stability and high electrocatalytic selectivity for ORR.

[a]*State Key Laboratory of Electroanalytical Chemistry, Changchun Institute of Applied Chemistry, Chinese Academy of Sciences, 5625 Renmin Street, Changchun, Jilin 130022, China. E-mail: youty@ciac.jl.cn*

[b]*University of Chinese Academy of Sciences, 19A Yuquan Road, Beijing 100049, China*

[c]*State Key Laboratory of Luminescence and Applications, Changchun Institute of Optics, Fine Mechanics and Physics, Chinese Academy of Sciences, 3888 East Nanhu Road, Changchun, Jilin 130033, China*

† Electronic supplementary information (ESI) available: Experimental and characterization details; SEM, contact angles of CNFs-A, CNFs-B and NCNFs; rotating disk electrode voltammograms and Koutecky–Levich plots of CNFs-A and CNFs-B; rotating ring-disk electrode voltammograms of NCNFs and Pt/C; and the electrocatalytic selectivity of the NCNFs and Pt/C. See DOI: 10.1039/c3nr03229a

Results and discussion

The free-standing NCNF films were synthesized by thermal treatment of electrospun PAN nanofibers in a high temperature furnace, and the thermal process was carried out in a capsule-shaped device composed of two combustion boats to fully utilize the tail gas for surface treatment (Scheme 1). Briefly, the electrospun PAN nanofibers were handled completely in nitrogen as follows: (1) stabilized at 300 °C for 60 min and (2) further carbonized at 900 °C for 60 min and then cooled to room temperature. For comparison, CNFs-A and CNFs-B were prepared in one combustion boat *via* the same process except for the first step for CNFs-A which were stabilized in air (Table S1†).

As observed from images of TEM and SEM (Fig. 1a–c and S1a–c†), the NCNFs (204 ± 26 nm) have not only a smaller diameter than CNFs-A (289 ± 12 nm) and CNFs-B (404 ± 35 nm), but also a rougher surface. Several nitrogen-containing gaseous compounds, such as NH_3 and HCN, were formed as byproducts in thermal treatment of PAN.[21] Then, the radicals that originated from the decomposition of NH_3 at high temperature, such as NH and NH_2, would etch the surface of carbon nanomaterials leading to the decrease of the diameter and the increase of the surface area.[22]

The Raman spectra of all samples displayed the D band (around 1340 cm^{-1}) and G band (around 1600 cm^{-1}) as shown in Fig. 2a. The intensity ratio of D band and G band (I_D/I_G) for NCNFs was calculated to be 1.93, which was higher than that of CNFs-A (1.85) and CNFs-B (1.87). Accordingly, the as-obtained results demonstrated that the graphitization degree of CNFs was higher than that of NCNFs. This may be attributed to the more structural defects and edge plane generated by the incorporation of nitrogen into the carbon matrix.[17,23] As a result, the NCNF films revealed significant hydrophilic behavior (Fig. S1e and f†).[24]

The X-ray photoelectron N1s spectra of CNFs-A, CNFs-B and NCNFs (Fig. 2b–d) demonstrated that the pyrrolic-N content (at.%) was 31.6, 35.2 and 44.1%, respectively. The NCNFs contained the highest content of pyrrolic structures, as a result of the reaction between the carbon host and H atoms or other H containing radicals generated by the decomposition of NH_3 during the carbonization.[19] It has already been reported that carbons with pyrrolic-N at the edges of graphene layers would exhibit higher charge mobility and better donor–acceptor properties than other kinds of nitrogen species, such as pyridinic-N and graphitic-N.[25]

The free-standing NCNF films exhibited many attractive properties, including rough surface, high content of pyrrolic-N and good hydrophilicity, which were expected to enhance its catalytic performance. In our work, the electrocatalytic activity of NCNFs was evaluated by ORR in the 0.1 M KOH solution, and further compared with other catalysts (Fig. 3). The NCNF films can be directly and stably adhered to the surface of a glassy carbon electrode by 0.5 wt% nafion solution (Fig. 1d). The ORR onset potential and peak potential at NCNFs were −0.034 V and −0.182 V, significantly more positive than those at CNFs-A (−0.120 V and −0.278 V) and CNFs-B (−0.154 V and −0.413 V), indicating much faster electron transfer kinetics and higher catalytic activity for ORR.

To gain further insight into the electrocatalytic properties of NCNFs and CNFs, rotating disk electrode (RDE) measurements were carried out. The RDE linear sweeping voltammograms with a rotation rate of 1600 rpm are displayed in Fig. 3b, and similar trends of the onset potential in ORR were obtained. The onset potential of NCNFs was about 45 mV more negative than

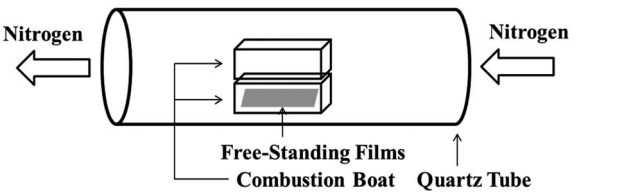

Scheme 1 The preparation of NCNFs in a capsule-shaped device composed of two combustion boats.

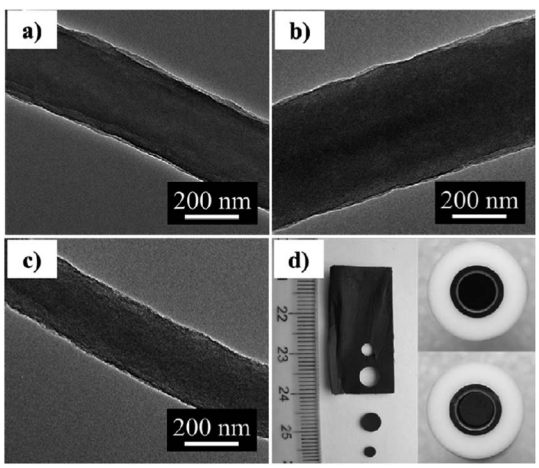

Fig. 1 TEM images of (a) CNFs-A, (b) CNFs-B and (c) NCNFs. (d) Photograph of free-standing NCNF films and disk-shaped NCNF films for the electrode modification.

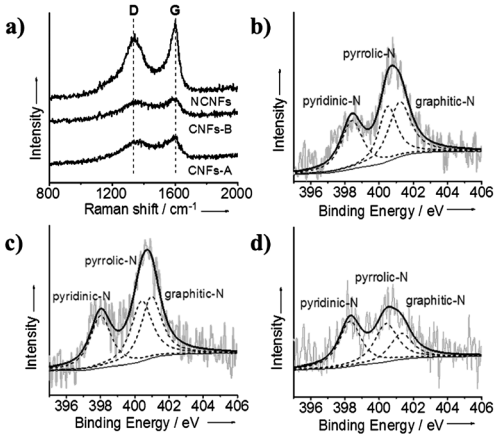

Fig. 2 (a) Raman spectra of CNFs-A, CNFs-B and NCNFs. X-ray photoelectron N1s spectra of (b) CNFs-A, (c) CNFs-B and (d) NCNFs.

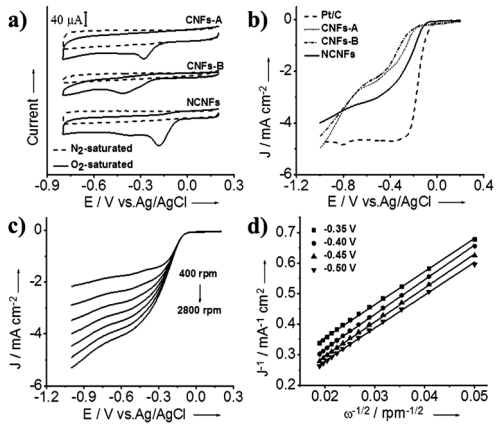

Fig. 3 (a) Cyclic voltammograms (CVs) of CNFs-A, CNFs-B and NCNFs in O_2- and N_2-saturated 0.1 M solution of KOH at a scan rate of 50 mV s^{-1}. (b) Rotating disk electrode voltammograms of CNFs-A, CNFs-B, NCNFs and Pt/C in O_2-saturated 0.1 M solution of KOH at a scan rate of 10 mV s^{-1} at 1600 rpm. (c) Rotating disk electrode voltammograms recorded for NCNFs in O_2-saturated 0.1 M solution of KOH at different rotation rates with a sweep rate of 10 mV s^{-1}. (d) Koutecky–Levich plot of J^{-1} *versus* $\omega^{-1/2}$ at different electrode potentials. The experimental data were obtained from (c).

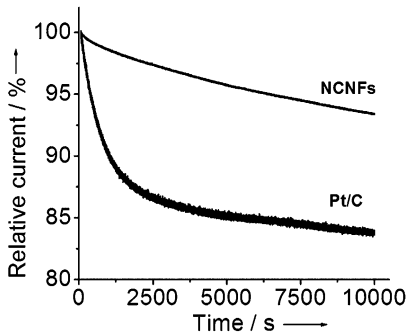

Fig. 4 Chronoamperometric response of NCNFs and Pt/C at −0.26 V in O_2-saturated 0.1 M KOH at a RDE rotation rate of 1600 rpm.

that of the Pt/C catalyst, suggesting high catalytic activity of NCNF films toward ORR. The electrochemical reduction of oxygen in basic solution includes two main possible pathways, involving the two-electron reduction pathway with OOH^- as an intermediate product and the four-electron pathway to produce OH^-.[26,27] The latter pathway is more desirable for the purpose of achieving the maximum energy capacity. To investigate the kinetic reaction mechanism of the electron process, the Koutecky–Levich equations were employed to calculate the number of electrons transferred (n) per oxygen molecule in the ORR.[28]

The n value calculated in the ORR for NCNFs was about 3.6–4.0 in the potential range from −0.35 V to −0.5 V (Fig. 3c and d), revealing that the electrocatalytic process of ORR at NCNFs is a close four-electron pathway leading to the direct formation of OH^-. In contrast, the n value was obtained to be 3.2–3.6 and 2.7–2.9 for CNFs-A and CNFs-B, respectively (Fig. S2†).

In order to investigate the percentage of peroxide species formed ($y_{peroxide}$) in the O_2-reduction procedure, we also performed the rotating disk-ring electrode (RRDE) measurements. The n value was calculated to be 3.52 for NCNFs at −0.5 V, and the value of $y_{peroxide}$ was measured to be 24% (Fig. S3†).[14]

$$n = 4I_D/(I_D + (I_R/N)) \quad (1)$$

$$y_{peroxide} = 100(4 - n)/2 \quad (2)$$

where N is the collection efficiency with a value of 0.37 and I_D and I_R are the faradic-disk and -ring currents. The n value from RRDE results was in agreement with that obtained from RDE measurements, demonstrating that the ORR at the NCNFs was mainly *via* the four-electron pathway.

The above observed excellent electrocatalytic activity of NCNFs toward ORR can be explained by the nitrogen-induced charge delocalization and high hydrophilicity.[15,29] The unique electronic properties of NCNFs derived from nitrogen inclusion may benefit the oxygen reduction.[15] In addition, the high hydrophilicity is expected for the efficient oxygen absorption and reduction.[29]

Because the stability of electrocatalysts is one of the major issues limiting the current fuel cell technology for practical applications, the durability of NCNFs was further measured at −0.26 V for 10 000 s in O_2-saturated 0.1 M KOH solution at a rotation rate of 1600 rpm (Fig. 4). Compared with the commercial Pt/C, the corresponding chronoamperometric response of NCNFs showed slow attenuation. The ORR current density of NCNFs exhibited a slight drop of 6.6% after a continuous operation of 10 000 s, while it dropped over 16.3% for commercial Pt/C, revealing an enhanced long-time stability of NCNFs for ORR. In addition to the durability, the electrocatalytic selectivity of the catalyst was another key issue to be investigated in ORR. To test the possible crossover, the ORR activity of NCNFs was explored in the presence of 3 M methanol. It showed that the electrocatalytic activity of NCNFs in ORR remained unchanged after the addition of methanol (Fig. S4a†), while a pair of peaks for methanol oxidation, located at −0.13 and −0.22 V, were observed in the CV curve of Pt/C, leading to the vanishing of the cathodic peak for ORR (Fig. S4b†). It has been reported that the high selectivity and remarkably good tolerance to the crossover effect can be attributed to the much lower ORR potential than that required for the oxidation of methanol.[15]

Conclusions

For the first time, free-standing NCNF films were prepared using the tail gas generated in the thermal treatment procedure for nitrogen doping and surface etching. The resultant NCNF films exhibited high catalytic activity, enhanced durability and high electrocatalytic selectivity toward ORR. Our work presents a potential approach for the large-scale production of NCNFs as an alternative to the Pt-based catalysts in the practical application of fuel cells.

Acknowledgements

We are grateful for the financial support from the National Natural Science Foundation of China (no. 21222505).

Notes and references

1 B. C. H. Steele and A. Heinzel, *Nature*, 2001, **414**, 345–352.
2 J. L. Shui, C. Chen and J. C. M. Li, *Adv. Funct. Mater.*, 2011, **21**, 3357–3362.
3 Z. W. Chen, D. Higgins, A. P. Yu, L. Zhang and J. J. Zhang, *Energy Environ. Sci.*, 2011, **4**, 3167–3192.
4 F. Jaouen, E. Proietti, M. Lefévre, R. Chenitz, J. Dodelet, G. Wu, H. T. Chung, C. M. Johnston and P. Zelenay, *Energy Environ. Sci.*, 2011, **4**, 114–130.
5 D. H. Deng, L. Yu, X. Q. Chen, G. X. Wang, L. Jin, X. L. Pan, J. Deng, G. Q. Sun and X. H. Bao, *Angew. Chem., Int. Ed.*, 2013, **52**, 371–375.
6 Y. Y. Liang, H. L. Wang, J. G. Zhou, Y. G. Li, J. Wang, T. Regier and H. J. Dai, *J. Am. Chem. Soc.*, 2012, **134**, 3517–3523.
7 Z. S. Wu, S. B. Yang, Y. Sun, K. Parvez, X. L. Feng and K. Müllen, *J. Am. Chem. Soc.*, 2012, **134**, 9082–9085.
8 Y. M. Yu, J. H. Zhang, C. H. Xiao, J. D. Zhong, X. H. Zhang and J. H. Chen, *Fuel Cells*, 2012, **12**, 506–510.
9 D. S. Yang, D. Bhattacharjya, S. Inamdar, J. Park and J. S. Yu, *J. Am. Chem. Soc.*, 2012, **134**, 16127–16130.
10 L. J. Yang, S. J. Jiang, Y. Zhao, L. Zhu, S. Chen, X. Z. Wang, Q. Wu, J. Ma, Y. W. Ma and Z. Hu, *Angew. Chem., Int. Ed.*, 2011, **50**, 7132–7135.
11 R. L. Liu, D. Q. Wu, X. L. Feng and K. Müllen, *Angew. Chem., Int. Ed.*, 2010, **49**, 2565–2569.
12 W. Yang, T. P. Fellinger and M. Antonietti, *J. Am. Chem. Soc.*, 2011, **133**, 206–209.
13 Z. H. Sheng, L. Shao, J. J. Chen, W. J. Bao, F. B. Wang and X. H. Xia, *ACS Nano*, 2011, **5**, 4350–4358.
14 D. S. Geng, Y. Chen, Y. G. Chen, Y. L. Li, R. Y. Li, X. L. Sun, S. Y. Ye and S. Knights, *Energy Environ. Sci.*, 2011, **4**, 760–764.
15 K. P. Gong, F. Du, Z. H. Xia, M. Durstock and L. M. Dai, *Science*, 2009, **323**, 760–764.
16 P. H. Matter, L. Zhang and U. S. Ozkan, *J. Catal.*, 2006, **239**, 83–96.
17 S. Maldonado and K. J. Stevenson, *J. Phys. Chem. B*, 2005, **109**, 4707–4716.
18 L. F. Chen, X. D. Zhang, H. W. Liang, M. G. Kong, Q. F. Guan, P. Chen, Z. Y. Wu and S. H. Yu, *ACS Nano*, 2012, **6**, 7092–7102.
19 Y. J. Qiu, J. Yu, T. N. Shi, X. S. Zhou, X. D. Bai and J. Y. Huang, *J. Power Sources*, 2011, **196**, 9862–9867.
20 H. P. Cong, X. C. Ren, P. Wang and S. H. Yu, *Energy Environ. Sci.*, 2013, **6**, 1185–1191.
21 F. A. Bell, R. S. Lehrl and J. C. Robb, *Polymer*, 1971, **16**, 579–599.
22 X. Q. Wang, J. S. Lee, Q. Zhu, J. Liu, Y. Wang and S. Dai, *Chem. Mater.*, 2010, **22**, 2178–2180.
23 Y. Liu, J. S. Huang, H. Q. Hou and T. Y. You, *Electrochem. Commun.*, 2008, **10**, 1431–1434.
24 S. Shanmugam and A. Gedanken, *J. Phys. Chem. B*, 2006, **110**, 2037–2044.
25 V. V. Strelko, V. S. Kuts and P. A. Thrower, *Carbon*, 2000, **38**, 1499–1524.
26 S. Kattel, P. Atanassov and B. Kiefer, *J. Phys. Chem. C*, 2012, **116**, 17378–17383.
27 L. Yu, X. L. Pan, X. M. Cao, P. Hu and X. H. Bao, *J. Catal.*, 2011, **282**, 183–190.
28 D. S. Yu, Q. Zhang and L. M. Dai, *J. Am. Chem. Soc.*, 2010, **132**, 15127–15129.
29 I. Y. Jeon, H. J. Choi, S. M. Jung, J. M. Seo, M. J. Kim, L. M. Dai and J. B. Baek, *J. Am. Chem. Soc.*, 2013, **135**, 1386–1393.